Journal of Thermal Analysis and Calorimetry
https://doi.org/10.1007/s10973-024-13361-8

Endo- and exothermal mechanocaloric response in rubbers

Takasuke Matsuo[1] · **Daisuke Takajo**[1]

Received: 23 November 2023 / Accepted: 29 May 2024

Abstract
We investigated mechanocaloric properties of two silicone rubbers using an in-house made apparatus. Tension f and temperature change ΔT of the rubber samples in the form of tapes were measured as they were extended up to a normalized length $\lambda \approx 2$ at a constant rate. Endothermal and exothermal components of the thermal response were observed and separated. The engineering stress and (decrease of) the entropy density derived from the data were analyzed. The number densities of the partial chains and the coefficients of the positive (endothermal) entropy contribution were determined as material constants of the rubbers. Non-idealities were revealed by the large difference between the work done on the rubber for the extension and the heat that evolved in the process. It decreased to a considerable extent when the heat was corrected for the endothermal effect arising from the above-mentioned endothermal entropy contribution. This may be understood as an indication of hidden near-ideality of silicone rubbers. Dissipation of the work into heat is quantified using the difference between the temperature changes on extension and contraction.

Keywords Rubber elasticity · Entropy of extension · Ideal rubber · Non-ideal rubber · Endothermal mechanocaloric effect · Exothermal mechanocaloric effect

Introduction

The temperature of a solid matter changes when it is deformed mechanically. The magnitude of the change is usually very small. Joule found back in 1859, using a sensitive device with a temperature resolution exceeding one mK, that the temperature of metals, alloys and other materials including various kinds of wood *decreased* when they were extended [1]. He found also that the temperature of the stretched material returned to the original value when the applied tension was removed. The thermal effect was reversible and hence belonged to the realm of thermodynamics which Joule was creating at that time with Kelvin and other scientists.

Rubber was exceptional among the substances Joule examined. The temperature change was opposite to that of other substances: The temperature of a rod of rubber *increased* when it was stretched and decreased when it was released back to the original length. He found also that the magnitude of the temperature change was much larger than those in other materials under the same experimental condition. This unusual mechanocaloric property of rubber is now known as an indication of the entropic origin of its elasticity.

There have been experimental works [eg. 2–4] dealing with mechanocaloric properties of rubber after Joule's experiment, but his work [1] was so carefully executed that it has been difficult to exceed and replace it for a long time.

In the meantime, rubber has become an important industrial material. New elastomers were synthesized and new experiments on mechanocaloric response [5, 6] and stress–strain relations reported [7, 8]. Theoretical analyses and further experiments on the stress–strain relation were also published [9, 10]. The developments both theoretical and experimental up to 1975 have been taken up in a monograph [11]. These comprise the bases of our understanding of the rubber elasticity. More recent developments in this field are incorporated in *soft matter physics* [12, 13]. We use, in the analysis of our experimental results below, these new formulations.

✉ Takasuke Matsuo
tmatsuo@bc4.so-net.ne.jp

Daisuke Takajo
takajo@chem.sci.osaka-u.ac.jp

[1] Research Center for Thermal and Entropic Science, Graduate School of Science, Osaka University, 1-1 Machikaneyama-cho, Toyonaka, Osaka, Japan

Published online: 31 July 2024

Recent developments in quantum chemistry, molecular dynamics and Monte Carlo simulations are beginning to produce results that can be compared with experimental data [14–16]. Also a new mathematical way of describing the state changes of elastomers has been developed to actually simulate the stress–strain relations [17]. An interesting problem in this direction is the distinction between adiabatic and isothermal changes of the state of an elastomer. It seems that even for a single polymer chain we do not know how to describe these changes at the molecular level. It is desirable to have new results on the experimental side in the mechanical and thermal aspects of the elastomer properties. The mechanocaloric coupling is also an interesting material property of a recent significance that it may be used in harvesting thermal energy from low level heat sources [18].

In the present paper, we describe an experiment which we performed recently on the mechanocaloric responses of two silicone rubbers of different hardness. We measured the temperature change and the tensile force on the rubber sample simultaneously as it underwent deformation, and derived the entropy of extension directly from the mechanocaloric effect. This allowed us to determine the heat and mechanical work involved in the deformation of the elastomers as a function of the extension. This type of experiment was started some time ago [19–21] and has since been improved with respect to the resolution of the measurement of the temperature and extension, and automatic recording of data. It has been further innovated by Suzuki and others [23] and combined with the heat capacity calorimetry for better understanding of the elasticity of rubber. In ICCT 2023, there have been presented four papers dealing with mechanocaloric (a.k.a. elastocaloric) properties of rubbers (https://www.chem.sci.osaka-u.ac.jp/lab/micro/icct2023/index.html).

Thermodynamic relations used in the analysis of the experimental data

In the approximation at the simplest level, the internal energy of a rectangular piece of rubber is given as follows.

$$\mathrm{d}U = T\mathrm{d}S + f\mathrm{d}L \tag{1}$$

where f and L are, respectively, the tensile force on the rubber sample and its length. The other symbols are used in the usual meaning. This form of the internal energy is justified on the ground that a typical rubber material becomes thinner in the directions perpendicular to the direction of extension, so as to keep the volume of the rubber approximately the same. Equation 1 resulted in a satisfactory explanation of the entropic origin of the rubber elasticity [11–13]. However, our experimental data have shown that we need a next level of approximation to take the volume change $\mathrm{d}V$ into account.

$$\mathrm{d}U = T\mathrm{d}S + f\mathrm{d}L - p\mathrm{d}V \tag{2}$$

In the approximation we employ here, we assume that the volume of a rubber increases when it is extended. This assumption is equivalent to a constant value of the Poisson ratio ν smaller than 1/2, and explains the endothermal mechanocaloric response as will be shown below.

The entropy is a function of T, L, and V. Its total differential is equal to zero for a quasi-static adiabatic extension:

$$\mathrm{d}S = 0 \tag{3}$$

where $\mathrm{d}S$ is written as follows.

$$\mathrm{d}S = \left(\frac{\partial S}{\partial T}\right)_{\mathrm{L,V}}\mathrm{d}T + \left(\frac{\partial S}{\partial L}\right)_{\mathrm{T,V}}\mathrm{d}L + \left(\frac{\partial S}{\partial V}\right)_{\mathrm{T,L}}\mathrm{d}V \tag{4}$$

This gives the following equation on division by $\mathrm{d}L$ at constant T and V.

$$\left(\frac{\partial S}{\partial T}\right)_{\mathrm{L,V}}\left(\frac{\partial T}{\partial L}\right)_{\mathrm{S,p}} + \left(\frac{\partial S}{\partial L}\right)_{\mathrm{T,V}} + \left(\frac{\partial S}{\partial V}\right)_{\mathrm{T,L}}\left(\frac{\partial V}{\partial L}\right)_{\mathrm{S,p}} = 0 \tag{5}$$

The temperature change in an adiabatic extension follows the next equation derived from Eq. 5.

$$\frac{C_{\mathrm{L,V}}}{T}\left(\frac{\partial T}{\partial L}\right)_{\mathrm{S,p}} = -\left(\left(\frac{\partial S}{\partial L}\right)_{\mathrm{T,V}} + \left(\frac{\partial S}{\partial V}\right)_{\mathrm{T,L}}\left(\frac{\partial V}{\partial L}\right)_{\mathrm{S,p}}\right) \tag{6}$$

where the relation $C_{\mathrm{L,V}} = T\left(\frac{\partial S}{\partial T}\right)_{\mathrm{L,V}}$ is used, with $C_{\mathrm{L,V}}$ defined as the heat capacity at constant length and constant volume. Equation 5 is further rewritten as follows.

$$\frac{C_{\mathrm{L,V}}}{T}\left(\frac{\partial T}{\partial L}\right)_{\mathrm{S,p}} = -\left(\left(\frac{\partial S}{\partial L}\right)_{\mathrm{T,V}} + \frac{\left(\frac{\partial S}{\partial p}\right)_{\mathrm{T,L}}}{\left(\frac{\partial V}{\partial p}\right)_{\mathrm{T,L}}}\left(\frac{\partial V}{\partial L}\right)_{\mathrm{S,p}}\right) \tag{7}$$

Substitution of a Maxwell relation $\left(\frac{\partial S}{\partial p}\right)_{\mathrm{T,L}} = -\left(\frac{\partial V}{\partial T}\right)_{\mathrm{p,L}}$ in Eq. 7 gives

$$\frac{C_{\mathrm{L,V}}}{T}\left(\frac{\partial T}{\partial L}\right)_{\mathrm{S,p}} = -\left(\left(\frac{\partial S}{\partial L}\right)_{\mathrm{T,V}} - \left(\frac{\partial V}{\partial T}\right)_{\mathrm{p,L}}\left(\frac{\partial p}{\partial V}\right)_{\mathrm{T,L}}\left(\frac{\partial V}{\partial L}\right)_{\mathrm{S,p}}\right) \tag{8}$$

The LHS of Eq. (8) is the experimental measure of the *decrease* of the entropy of the rubber that occurs when it is extended isothermally (see Eq. 21 below). The first term in the parentheses on RHS represents the decrease of the entropy that occurs in the rubber as it is stretched isothermally at a constant volume. This is the main part of the thermal effect of the rubber elasticity and is often taken up in thermodynamics courses to introduce the entropy

as a measure of disorder. The second term describes the effect of extension on the entropy through the change in the volume that accompanies extension. The third factor of the second term gives the volume change of the rubber for a given extension, while the first and second factors together translate the volume change to the entropy change. The first factor is in a form similar to but not equal to the thermal expansion coefficient, $\alpha = (1/V)(\partial V/\partial T)_{\mathrm{p}}$. The second factor is again in a form similar to but not equal to the bulk modulus $K = -V(\partial p/\partial V)_{\mathrm{T}}$. The difference lies in that the corresponding partial differentiations in Eq. 8 are taken under an additional restriction $L =$ constant.

The third factor $(\partial V/\partial L)_{\mathrm{S,p}}$ is rewritten in a form involving Poisson's ratio as follows.

A rectangular rubber sample of volume $V = abL$ is extended to a length $L + \Delta L$. The sides are reduced to $a - \Delta a$ and to $b - \Delta b$. Change of the volume ΔV is written as follows,

$$\Delta V = (a - \Delta a)(b - \Delta b)(L + \Delta L) - abL$$

$$\approx ab\Delta L - aL\Delta b - bL\Delta a \tag{9}$$

$$\frac{\Delta V}{\Delta L} = -aL\frac{\Delta b}{\Delta L} - bL\frac{\Delta a}{\Delta L} + ab \tag{10}$$

$$\approx -2ab\nu + ab = ab(1 - 2\nu) \tag{11}$$

Poisson's ratio ν is defined as follows

$$\nu = \frac{(\Delta a)/a}{(\Delta L)/L}, \quad \Delta L \to 0 \tag{12}$$

A similar relation holds with b in place of a. Equation 11 shows that the volume of a material with Poisson's ratio ν equal to 0.5 remains the same when it is extended, whereas the volume of those materials with $\nu < 0.5$ increases when they are extended.

In the above derivation, we disregarded the possible difference in the volume changes arising from adiabatic and isothermal changes of its length. In the analysis described below, this difference is absorbed in one of the least-squares parameter along with two other material constants (see Eq. 27).

The coupling Eq. 11 between L and V has an effect on the force given by the partial derivative of the Helmholtz energy with respect to L.

$$\left(\frac{\partial F}{\partial L}\right)_{\mathrm{T}} = f - pab(1 - 2\nu) \tag{13}$$

The second term arises from the coupling between L and V. Typical values in the our experiment are $f = 1 \sim 20$ N and $ab = 20$ mm^2. For $\nu = 0.4999$(a reported value for natural rubber [24]), the correction term is equal to 0.0004 N and easily negligible in comparison with the force $f = 1 \sim 20$ N

Equation 8 is rewritten in Eq. 14 by introducing these material constants. The primes on α and K indicate that these are partial derivatives taken under an additional restriction of constant L.

$$\frac{C_{\mathrm{L,V}}}{T}\left(\frac{\partial T}{\partial L}\right)_{\mathrm{S,p}} = -\left(\left(\frac{\partial S}{\partial L}\right)_{\mathrm{T,V}} + \alpha' K' ab(1 - 2\nu)\right) \tag{14}$$

Further introduction of a normalized length variable $\lambda = L/L_0$ where L_0 is the initial length of the sample and division by $V = abL_0$ changes Eq. 14 to the following form.

$$\frac{c_{\lambda,\mathrm{V}}}{T}\left(\frac{\partial T}{\partial \lambda}\right)_{\mathrm{S,p}} = -\left(\left(\frac{\partial s}{\partial \lambda}\right)_{\mathrm{T,V}} + \alpha' K'(1 - 2\nu)\right) \tag{15}$$

Here the heat capacity $c_{\lambda,\mathrm{V}}$ and entropy s are respective quantities per unit volume of rubber. The experimental data presented below are analyzed using Eq. 15.

Experimental apparatus

General

The sample, a pair of ca.70-mm-long tapes of rubber (see below for details) is held together in a temperature-stabilized 20x20x55 cm^3 wooden box shown in Fig. 1. The upper end of the sample is hooked on a force gauge and the lower end connected to the upper end of a rack whose vertical position is controlled precisely and reproducibly by rotation of a meshing pinion. The axle of the pinion is rotated by a pulley driven by an adjustable-speed motor. The force gauge and pinion-and-rack mechanism are, respectively, situated above and below the top and bottom plates of the temperature-stabilized box, the force being transmitted to the rubber by connecting wires through the plates.

The mechanical part of the apparatus has to be rigid and stable as it determines the accuracy, precision and reproducibility of the measurement of the sample length. This is achieved by a sturdy wooden bar (120x5x1.5 cm^3) on which the force gauge and the bearing of the pinion are screwed firmly. The wooden bar itself is held firmly to an iron frame forming the entire sample environment. The wooden box surrounding the sample is held in position with its upper and lower plates fixed to the central wooden bar.

Measurement of the length of the sample

A ten-turn 10 kΩ potentiometer is coupled with the axle of the pinion. Extension of the sample rubber, determined by the vertical position of the rack, is encoded accurately

Fig. 1 The thermostated sample space shown with the front panel removed

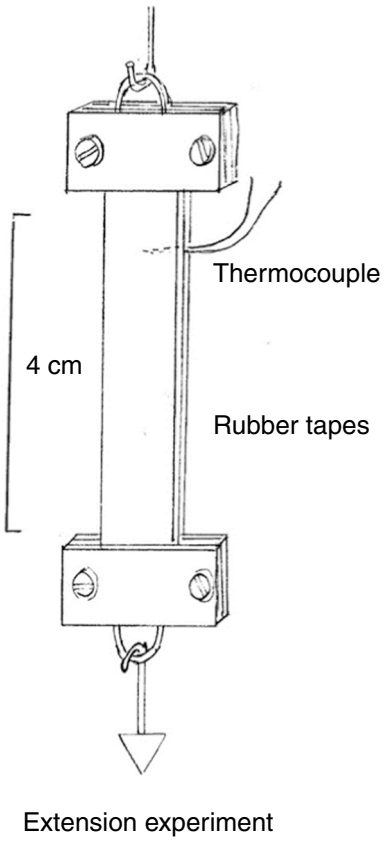

Fig. 2 The sample

on the resistance of the potentiometer. The relation between the potentiometer resistance and length of the sample was calibrated by actually measuring the vertical position y of the rack as a function of the potentiometer resistance x. y was read against a ruler and x measured by a DMM. For the calibration, 26 points were taken in the range 10.3 mm $< y <$ 42.9 mm. Corresponding resistances were 82 Ω $< x <$ 771 Ω. The position y was a good linear function of x, the maximum deviation from the best-fit line being 0.19 mm and the correlation coefficient between x and y 0.999963. The coefficient relating the length to the potentiometer resistance was 0.0470 mm/Ω. This value was used in the calculation of the sample length from the heliport resistance value. The effective diameter of the pinion calculated from this coefficient was 14.96 mm against the nominal diameter 15.0 mm.

The sample (Fig. 2) is typically two 70-mm-long tapes of rubber with 10 to 15 mm width and 0.5 or 1.0 mm thickness (depending on the material available for the experiment). Two clips, made of 10x15 mm^2 pieces of stainless steel, a phosphorus bronze plate spring of a similar size and two pairs of screws, are attached to both ends of the sample using the 10 mm end portions of the tapes. The effective length of the sample is ca. 50 mm.

The sample suspended down along the center bar is covered with an aluminum and acryl plate box (50x40x300 mm^3) for better thermal stability of the sample environment. The tension on the sample is transmitted by stainless steel wires through the holes in the end plates of the aluminum box.

The temperature of the air circulated in the wooden box by a fan is stabilized by a thermistor-controlled heating circuit (maximum 20 W). The air in the aluminum and acryl plate box, which is in direct contact with the sample and the reference junction of the thermocouple, is gently circulated with a smaller fan.

Measurement of the deformation, force and temperature

Three quantities are measured: the extension of the sample, the tension on it and its temperature change. The extension of the sample is translated precisely to the resistance of a potentiometer by a rack-and-pinion mechanism, as described in the previous section. The resistance is measured by a

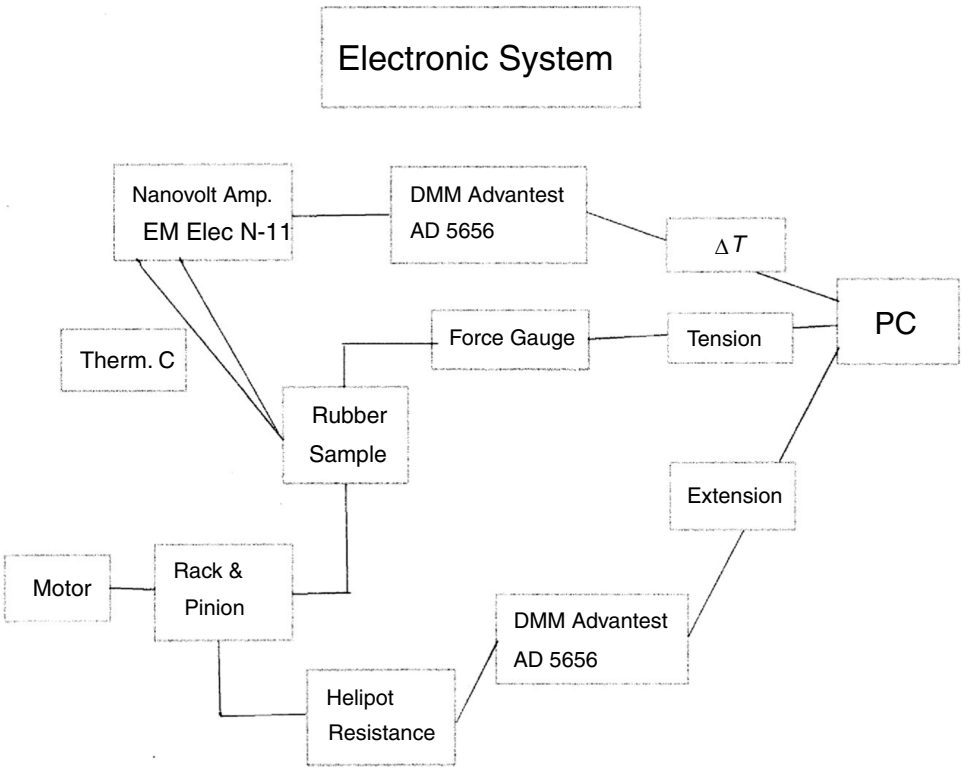

Fig. 3 The data acquisition and recording system

digital multimeter (DMM) to 0.1 Ω while 1 Ω is the precision needed. The entire system is shown in Fig. 3 in a block diagram.

The force on the sample is measured with a digital force gauge to 0.01 N, the zero of the force being taken as the mass of the rubber and two connecting clips. The initial length of the sample is somewhat indeterminate because of warping of the sample and irregularity in the fastening at the clips. This was corrected for by back extrapolation of the force vs. extension curve to the zero of the force.

For the measurement of the sample temperature, a chromel vs. constantan thermocouple (each 50 μm diameter) is inserted between the tapes of the rubber sample. The thermocouple voltage relative to the reference junction attached to the central bar (see above) and covered with a piece of copper plate is lead to an analog nanovolt amplifier, amplified by a factor of 1000 and measured on a DMM. The noise amplitude is typically (±)3 nanovolt at a sampling interval of 0.5 s, corresponding to a noise level of about 50 μK.

These three digitized quantities (force, heliport resistance and thermocouple output signal) are recorded on a computer as functions of time using a LabVIEW software.

The samples

Silicone Rubber1: Manufactured by WAKI Sangyo, Osaka, Japan, bought in 2020. It was cut in tapes 10.1 mm wide and 70 mm long. Two of them were held together and their ends caught by clips. The thickness of the two tapes were 2.1 mm. The effective length was 53 mm. Chemical analysis is not available.

Silicone Rubber 2: Manufactured by Shin-etsu Silicone, bought in 2014. It was used in the experiment reported in 2016 [21] and had been kept in a dark place. It was cut in tapes, width 12.0 mm and length 70 mm, thickness 1.0 mm in double. The effective length was 51 mm. Chemical analysis gave 2.88:1 for the number ratio H:C vs. the ideal value of 3:1.

Experimental procedure

When the sample was set up in the apparatus, the three quantities were recorded properly and the temperature sufficiently stable, the sample was extended at a chosen speed. The tensile force increased and the temperature *decreased* for a short time. If the extension was continued, the temperature changed to increasing and continued to increase until the extension was stopped at the desired length of the rubber. The length of the sample was kept constant for some time while the tension and temperature were continually recorded. The tension decreased exponentially for a short time just after the extension was stopped, indicating a process of relaxation taking place in the stressed rubber. The magnitude of the relaxation was ca. 0.3 N when the tension was 15 N (close to the largest

tension in the present experiment for Silicone 1). We took, as the equilibrium tension corresponding to the length of the sample recorded, the tension value read when the transient effect had died out.

When the transient change of the force became sufficiently small and the trend of the temperature change was recorded sufficiently stably, the motor driving the pinion was turned on in reverse to decrease the sample length to the original value. The tension decreased, and the temperature also decreased (if the extension had been sufficiently large), reached a minimum and then approached the final value from below. The measurement was continued for a while to record the trend of the temperature change. This concluded one cycle of measurement in which a triple of data, the length, tension and temperature were determined. The cycle of measurement may be repeated with a different value of extension, or the measurement may be ended.

The length of the sample L is usually given in a reduced form $\lambda = L/L_0$ where L_0 is the length of the sample in the free state. The force f is also normalized to the unit sectional area A_0 of the *unstrained* sample. The stress thus normalized is known as the engineering stress. $\sigma_e = f/A_0$. Extensions up to $\lambda = 2.0$ and 2.5 were studied for Silicone 1 and Silicone 2, respectively.

Experimental results

In Fig. 4 where a set of data on Silicone 1 is plotted, the upper trace shows the temperature change and the lower one the tension on the rubber sample both against time. The λ value is also given for each of the peaks. In this small λ region, the temperature decreased when the sample was extended. We notice that the response is very fast, almost instantaneous in the present experimental condition (two readings in a second). The fast response indicates that the temperature of the rubber decreases uniformly over the entire body of the sample, which means that heat conduction through rubber (a bad conductor of heat) is not involved in the thermal response process. The thermocouple is sensing the temperature of the rubber in direct contact with it.

At larger extensions, a positive temperature change becomes noticeable. Figure 5 shows the case in which the endothermal and exothermal effects closely balance out. We show below that the magnitude of the endothermal effect is proportional to $(\lambda - 1)$, whereas the exothermal effect to $(\lambda - 1)^2$. Hence, the positive effect becomes increasingly stronger at larger extensions. In Fig. 5, the decreasing part of the first dip of the temperature corresponds to the endothermal effect that became gradually canceled out by the exothermal effect as λ increased. The central portion of the curve corresponds, at $\lambda = 1.296$, to the equilibrium temperature which happened to be the same as the temperature at which the sample had been in equilibrium in the un-stretched state. The temperature decreased slightly with time for a reason not known at present. The second dip of the temperature in Fig. 5 shows the temperature of the rubber tracing back the course of the temperature change in the opposite direction as λ decreased from 1.296 to 1.0. The similar shapes of the two dips can be taken as an indication of a good reproducibility and the quasi-static nature of the extension-contraction cycle.

The tension on the sample increased nonlinearly with time and decreased also nonlinearly, as shown by the lower trace in Fig. 5. The nonlinearity is more evident for larger

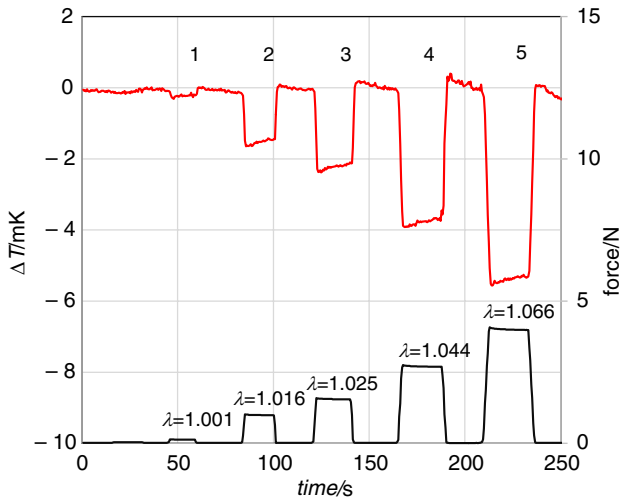

Fig. 4 Tension (the right scale) and temperature change of Silicone Rubber 1 undergoing extension/contraction in the small extension region. The temperature *decreases* on extension. Normalized length λ of the sample is indicated for each of the five peaks. Data: PDMSWAKIQQextAa02a, 20220802

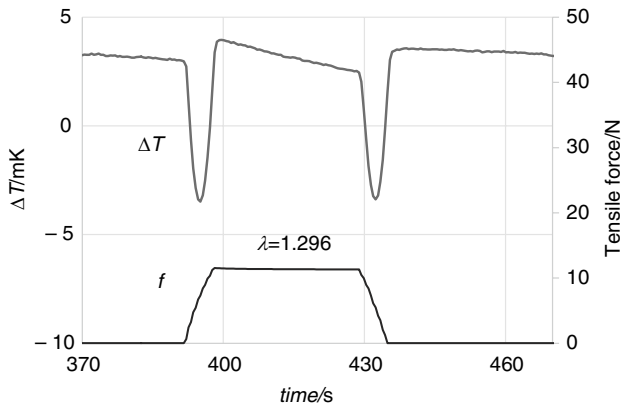

Fig. 5 Silicone Rubber 1. Traces of the temperature T (upper) and tensile force f (lower) vs. time. The sample was extended to $\lambda = 1.296$ and then released to $\lambda = 1.0$. The endo- and exothermal effects nearly cancel out at this extension. Data: PDMSWAKIQQextAa04a, 20220802

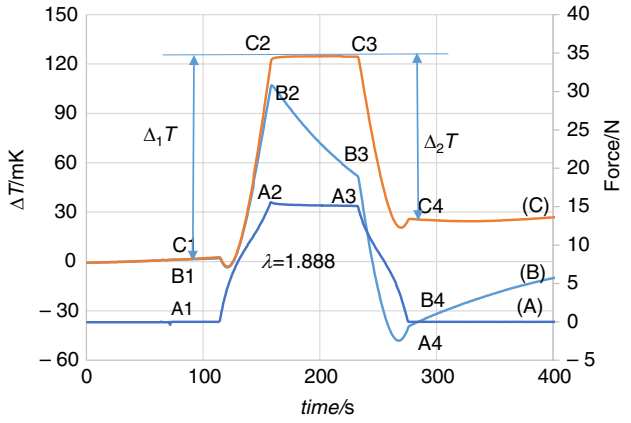

Fig. 6 Silicone Rubber 1. Definition of $\Delta_1 T$, $\Delta_2 T$ and special points on the curves of the tension **A**, the temperature **B** as observed, and the temperature **C** corrected for the heat leakage. Data: PDMSExthardAa14, 20220304

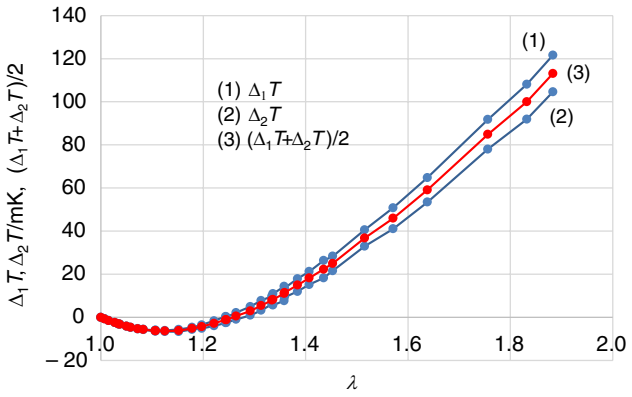

Fig. 7 Silicone Rubber 1. **1** $\Delta_1 T$ = temperature change on extension to λ, **2** $\Delta_2 T$ = the same on contraction back to $\lambda = 1.0$. The average **3** $(\Delta_1 T + \Delta_2 T)/2$ gives the magnitude of the reversible part of temperature change. The heat and entropy of extension are calculated therefrom. Data: PDMSExthardAa01a, 20220304

extensions. The nonlinearity is a general property of rubber as is discussed below (Eq. 19).

In Fig. 6, we plot three curves (A), (B) and (C) against time for an extension of Silicone 1 to $\lambda = 1.888$. Curve (A) is the force (tension) on the sample. Curve (B) is the sample's temperature change as measured and Curve (C) the temperature change corrected for the heat lost to the surrounding air. On each curve the point 1 marks the beginning of the extension, point 2 its end, point 3 the beginning of the contraction and point 4 its end.

The portion A1 to A2 is clearly curved. Since the time rate of the change of λ is constant (being driven by a constant speed motor), this arises from the nonlinear force law. A similar nonlinearity is seen also in the part of the curve A3-A4.

In order to determine the increase and decrease in temperature, $\Delta_1 T$ and $\Delta_2 T$, arising from the extension and contraction, respectively, the following correction was made to the observed temperature change Curve (B).

When the temperature of the sample is different from that of the surrounding air, the time rate of the temperature change due to the heat loss to the air follows the Newton's law:

$$\frac{\mathrm{d}\Delta T}{\mathrm{d}t} = -\frac{\Delta T - \Delta T_0}{\tau} \tag{16}$$

Here ΔT_0 is the convergence temperature and τ the time constant of the approach to the convergence temperature. This type of cooling law is appropriate as we have shown in [20]. The correction to be added to the observed temperature is given by the following numerical integration.

$$\delta\Delta T(t) = \sum_i \left(\frac{\mathrm{d}\Delta T}{\mathrm{d}t}\delta t\right)_i = \sum_i \left(\frac{\Delta T_0 - \Delta T}{\tau}\delta t\right)_i \tag{17}$$

Here $(\delta t)_i$ is the time interval between i-th and $(i+1)$-th measurement of the temperature, $(\delta t)_i \sim 0.5$ s in the present experiment. $\Delta T_0 = 0.00$ mK and $\tau = 102$ s were chosen in the following manner. The two portions of the curve B2-B3 and B4- were reproduced well by a single τ function separately with nearly equal sets of parameter values. We calculated the correction Eq. 17 for a few combinations of ΔT_0 and τ, and took the best one that reproduced the *nearly constant segments* in the curve C.

The three sections of the Curve C in Fig. 6 are separately constant so that the differences between them $\Delta_1 T = 123.2$ mK and $\Delta_2 T = 99.7$ mK were determined without much ambiguity.

Similar data were collected for different values of λ and corrected for the heat loss in the same way. Resulting $\Delta_1 T$,$\Delta_2 T$ and their averages $(\Delta_1 T + \Delta_2 T)/2$ are plotted in Fig. 7. They have the following physical meaning: $\Delta_1 T$ is the *sum* of the thermodynamic (quasi-static) increase of the temperature due to the mechanocaloric effect and the increase of the temperature arising from irreversible dissipation of the mechanical energy into thermal energy.$\Delta_2 T$ is the *difference* between these two thermal effects. If we assume that the irreversible heat effects in extension and contraction are the same, they are canceled out in the average $(\Delta_1 T + \Delta_2 T)/2$ of these two temperature changes. It gives the *reversible* thermodynamic temperature change due to the mechanocaloric effect. This quantity is related with the reversible entropy change of extension of the rubber.

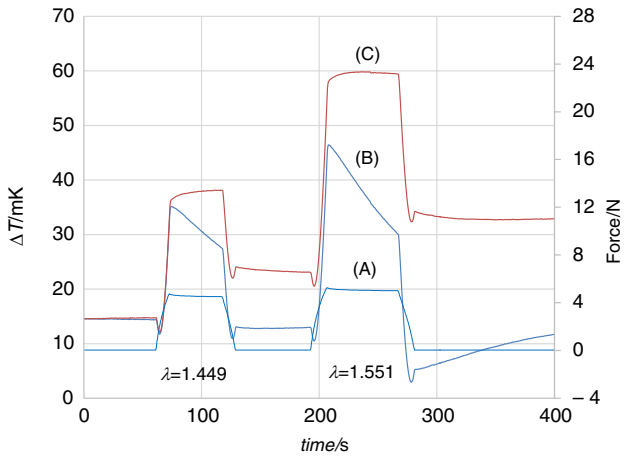

Fig. 8 Silicone Rubber 2. Curve **A** force, Curve **B** temperature as measured and **C** temperature corrected for the heat leakage to the air each for two runs to $\lambda = 1.449$ and 1.551. Data: pdmsBc03a, 20220411

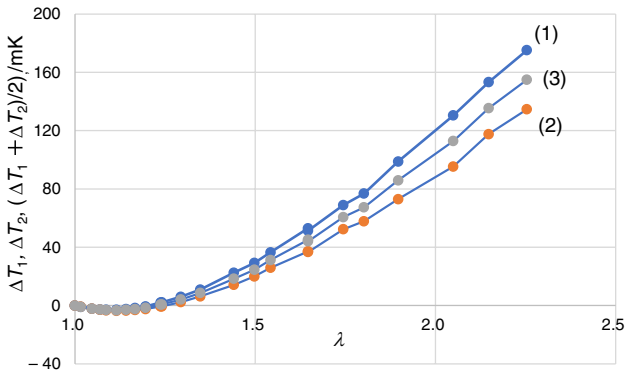

Fig. 9 Silicone Rubber 2. **1** $\Delta_1 T$ = temperature change of on extension to λ, **2** $\Delta_2 T$ = the same on contraction back to $\lambda = 1.0$. The average **3** $(\Delta_1 T + \Delta_2 T)/2$ gives the magnitude of the reversible part of temperature change. The heat and entropy of extension are calculated therefrom Data: pdmsBc07Analysis, 20220411 sheet2

$(\Delta_1 T - \Delta_2 T)/2$ represents the dissipative contribution to the temperature increase and will be discussed later by comparing it with the mechanical energy expended in the extension.

Figures 8 and 9 show the experimental results for Silicone Rubber 2. Figure 8 presents the force, temperature change as measured, and the corrected temperature change for $\lambda = 1.449$ and $\lambda = 1.551$. Figure 9 shows the temperature change for the whole region of the extension. We see from these four Figs. 6–9 that Silicone Rubber 1 and 2 behave in a similar way with regard to the mechanocaloric response.

Discussion

In the ideal rubber approximation, the entropy of a piece of rubber extended to λ is, for a unit volume, given by

$$s(\lambda) = -\frac{1}{2} n_c k(\lambda^2 + 2/\lambda - 3) \tag{18}$$

where n_c is the number density of partial chains forming the rubber and k the Boltzmann constant [11–13]. Equation 18 is negative for $\lambda > 1$ and gives the entropy of an extended rubber relative to its entropy in the free state where $\lambda = 1.0$.

The engineering stress $\sigma_e(\lambda)$(the stress not corrected for the change in the cross-sectional area) needed to extend a unit cube of rubber to λ in one direction is

$$\sigma_e(\lambda) = G(\lambda - 1/\lambda^2) \tag{19}$$

where

$$G = n_c kT \tag{20}$$

is the shear modulus [12, 13].

The stress strain relation

Figure 10 shows the engineering stress of Silicone 1 as a function of λ and two curves of the form Eq. 19 that try to reproduce the experimental data. The fitting is unsatisfactory with either parameter values, G=0.686 MPa or G=0.583 MPa optimized, respectively, for small λ values or for the entire region. Rather poor fitting was found also for natural rubber with the same fitting function [22]. G is related to n_c by $n_c = G/kT$; hence, the two G values are equivalent to $n_c = 1.69\text{E}+20$ /mL and $n_c = 1.44\text{E}+20$ /mL.

For Silicone 2, the results are qualitatively similar to those for Silicone 1. The best-fit G values are 0.290 and 0.256 MPa

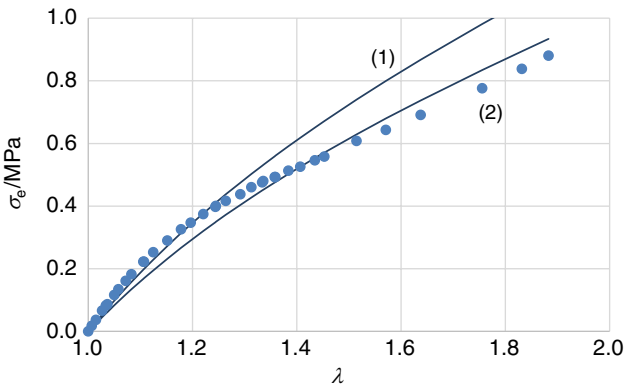

Fig. 10 Engineering stress σ_e *vs.* λ of Silicone Rubber 1 and its best-fit ideal rubber functions, $\sigma_e(\lambda) = G(\lambda - 1/\lambda^2)$, G=shear modulus Curve **1** G=0.686 MPa ($1 < \lambda < 1.3$), Curve **2** G=0.583 MPa ($1 < \lambda < 2.0$). Data: PDMSExthardAaAnalysB, 20220304

for the small λ and the entire λ regions, respectively. The smaller values of G of Silicone 2 than those of Silicone 1 correspond to Silicone 2 being softer than Silicone 1. In terms of n_c, Eq. (20) gives $n_c = 7.08\text{E}+19$/mL and $n_c = 6.28\text{E}+19$/mL for the small λ region and the entire λ region fitting.

The entropy of extension

The differential dS of the entropy is given by

$$\mathrm{d}S = \frac{\delta Q}{T} = \frac{C}{T}\mathrm{d}T = \frac{C_V}{T}\left(\frac{\partial T}{\partial L}\right)_{\mathrm{S,p}}\mathrm{d}L \tag{21}$$

The rightmost expression of this equation (with dL removed) is equal to the LHS of Eq. 14. Hence integration of Eq. 14 by dL gives the entropy change of the rubber that would occur if the evolving heat were *removed* from the rubber. For a unit volume of the rubber integration of the LHS of Eq. 15 from $\lambda = 1$ to $\lambda = \lambda$ gives the entropy density change of the rubber that occurs as it is extended from $\lambda = 1$ to λ.

$$s(\lambda) - s(1) = -\int_1^{\lambda} \frac{c_{\lambda,\mathrm{V}}}{T}\left(\frac{\partial T}{\partial \lambda}\right)_{\mathrm{S,P}}\mathrm{d}\lambda \tag{22}$$

$$\approx -\frac{c_{\lambda,\mathrm{V}}}{T}\Delta T(\lambda) \tag{23}$$

The integral in Eq. 22 is replaced by a single term. This is justified since the integrand is very closely constant in the interval of the integration where T is the temperature at which the experiment was performed (~ 300 K) and $\Delta T = 1$ K at most, while $c_{\lambda,\mathrm{V}}$ (the heat capacity density at constant λ and V) is represented well by a single value (assumed or derived from a separate experiment). Equation 23 is used to determine the change in the entropy density from the experimental data as shown in Figs. 7 and 9.

The specific heat capacity of Silicone 2 measured by A. Inaba (Private communication to T. Matsuo is gratefully acknowledged) is represented well by

$$c_{\mathrm{p}}(T)/(Jg^{-1}K^{-1}) = 1.4175 + 0.0936\left(\frac{T/K - 300}{50}\right) \tag{24}$$

for $250 \le T/\mathrm{K} \le 350$.

The mass density of silicone is assumed to be 1.01 g mL^{-1}. These data were substituted in Eq. 23 to calculate the entropy density from the temperature change data. The heat capacity c_V differs from the heat capacity c_{p} by 3 to 5 percent for most of the substances in condensed state, the latter being larger than the former [25]. This will have to be taken into account in a more detailed analysis of the present result.

A theoretical equation to be compared with the experimental entropy Eq. 23 is derived by integration of the RHS of Eq. 15.

$$-\int_1^{\lambda}\left(\left(\frac{\partial s}{\partial \lambda}\right)_{\mathrm{T,V}} + \alpha' K'(1-2\nu)\right)\mathrm{d}\lambda = \frac{1}{2}n_c k(\lambda^2 + 2/\lambda - 3) - \alpha' K'(1-2\nu)(\lambda - 1) \tag{25}$$

Here we use for the first term in the integrand the entropy density of an ideal rubber given by Eq. 18. Note that $s(1) = 0$.

The two constants on RHS of Eq. 25 are abbreviated as follows.

$$-\frac{1}{2}n_c k = A \tag{26}$$

$$\alpha' K'(1-2\nu) = B \tag{27}$$

The final form of the fitting equation is given by

$$-s(\lambda) = A(\lambda^2 + 2/\lambda - 3) - B(\lambda - 1) \tag{28}$$

Figure 11 shows the (negative) entropy density of Silicone 1 as a function of λ and the best-fit functions (Eq. 28) for a small-λ region (curve (1)) and the entire λ region (curve (2)). It is important that the irreversibility revealed by the difference between $\Delta_1 T$ and $\Delta_2 T$ has been taken into account. The best-fit parameter values are given in the caption of Fig. 11.

By rewriting RHS of Eq. 28 in the form $A(1/\lambda)(\lambda+2)(\lambda-1)^2 - B(\lambda-1)$, we see that the first

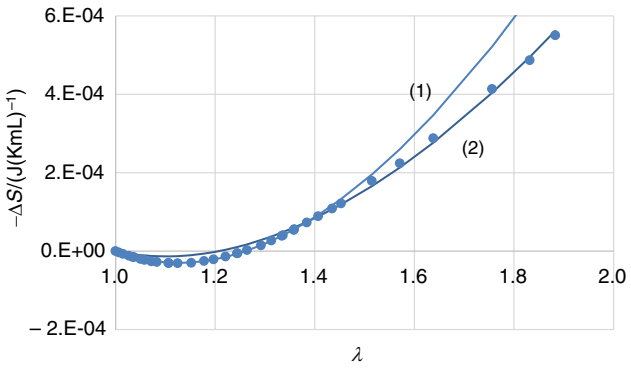

Fig. 11 Entropy of extension *vs.* λ of Silicone Rubber 1. Curve **1**, $1.0 < \lambda < 1.4$, $A = 7.33\text{E-}04$ J K^{-1} mL^{-1}, $B = -4.94\text{E-}04$ J/(K mL), $G = 0.431$ MPa, $n_c = 1.06\text{E}+20$ /mL. Curve **2**, $1.3 < \lambda < 2.0$, $A = 5.01\text{E-}04$ J K^{-1} mL^{-1}), $B = -2.76\text{E-}04$ J K^{-1} mL^{-1}), $G = 0.295$ MPa, $n_c = 0.726\text{E}+20$ /mL. G: shear modulus, n_c: number density of partial chains. Data: PDMSExthardAa01a, 20220304

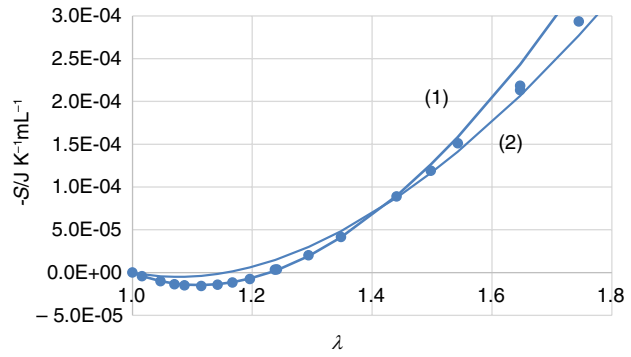

Fig. 12 Entropy of extension *vs.* λ of Silicone Rubber 2. Curve **1**, $1.0<\lambda<1.4$, $A=4.53\text{E-}04$ J K^{-1} mL^{-1}, $B=-2.73\text{E-}04$ J K^{-1} mL^{-1}, $G=0.268$ MPa, $n_c=6.56\text{E}+19$ /mL. Curve **2**, $1.3<\lambda<2.3$, $A=3.17\text{E-}04$ J/(K mL), $B=-1.35\text{E-}04$ J K^{-1} mL^{-1}), $G=0.188$ MPa, $n_c=4.59\text{E}+19$ /mL. G: shear modulus, n_c: number density of partial chains. Data: pdmsBc07a, 20220411 sheet2

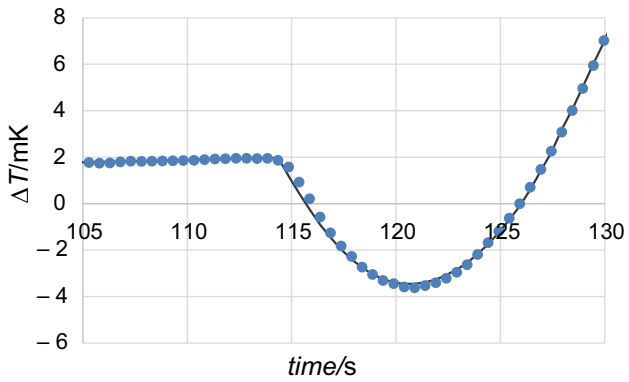

Fig. 13 An enlarged view of the first negative peak of the temperature vs. time plot for Silicone Rubber 1 in Fig. 6. The calculated curve is given by $\Delta T/\text{mK} = \text{Const.} + 146.1(\lambda(t)^2 + 2/\lambda(t) - 3) - 95.1(\lambda(t) - 1)$. By multiplication by the heat capacity density and division by the experimental temperature (294 K), the best-fit parameter 146.1 mK corresponds to $A = 7.12\text{E} - 04$ J(K^{-1} mL^{-1}) and -95.1 mK to $B = -4.63\text{E} - 04$ J(K^{-1} mL^{-1}). These agree with the best-fit values given in the caption of Fig. 11 for the small λ fitting. Data: PDMSExthardAa, sheet1 20220304

term is proportional to $(\lambda - 1)^2$ and the second term linear in $(\lambda - 1)$. This makes them separable in the fitting to a second order polynomial in $(\lambda - 1)$, as we have done in Fig. 11.

Figure 12 is a similar presentation of the entropy change of Silicone Rubber 2. The best-fit values of the parameters are similarly given. By comparing Figs. 11 and 12, we recognize that the harder rubber (Silicone 1) has a larger value of n_c than the softer one, which means that the partial chains are shorter in harder Silicone 1 than in softer Silicone 2.

In the previous section, we discussed the stress–strain relation. There we considered only the ideal rubber term of the free energy disregarding in effect the B-term defined above by Eq. 27. This is justified because the B-term contributes to the free energy through the entropy and the internal energy in the opposite ways canceling each other.

Reproducing the temperature–time relation

Figure 13 shows a part of the temperature–time relation given in Fig. 6 in a larger scale. It shows the part of the experimental curve where the temperature decreases just after the beginning of the extension. It also shows a calculated curve that reproduces the experimental data. The essential part of the curve, excluding the slightly sloping base line, is calculated by the following equation.

$$\Delta T(t)/\text{mK} = 146.1(\lambda(t)^2 + 2/\lambda(t) - 3) - 95.1(\lambda(t) - 1) \tag{29}$$

The two numerical constants are determined by the least-squares fitting. Notice that Eq. 29 is a function of time through $\lambda = \lambda(t)$. As shown in the caption of Fig. 13, the parameters determined here agree satisfactorily with those from the analysis of the entropy vs. λ curve (Fig. 11), specifically with the result from the small λ region, i.e., the curve (1): The small λ region in Fig. 13 corresponds to the first negative peak of the temperature in Fig. 6.

Comparison of the mechanical energy expended in the extension and the heat that evolves

One of the features of the present experiment is that we measure simultaneously the mechanical work expended on the sample for extension and the heat that evolves in the process. We compare these energy components comprising the internal energy of the rubber.

The mechanical energy density $W(\lambda)$ was calculated by numerical integration of $\sigma_e(\lambda)$ with respect to λ in the form of trapezoidal summation.

$$W(\lambda) = \sum_i \sigma_e(\lambda_i) d\lambda_i \tag{30}$$

and the heat density $Q(\lambda)$ by

$$Q(\lambda) = c_{\lambda,V} < \Delta T > \tag{31}$$

Equation 31 is analogous to Eq. 23 but without T in the denominator and with a suitably chosen sign.

Figure 14 shows the two energy components $W(\lambda)$ and $Q(\lambda)$ vs. λ of Silicone Rubber 1 and Fig. 15 a similar plot for Silicone Rubber 2. For both of the rubbers, the mechanical energy expended is considerably larger than the heat that evolves. The difference is stored in the rubber. They are thus non-ideal rubbers.

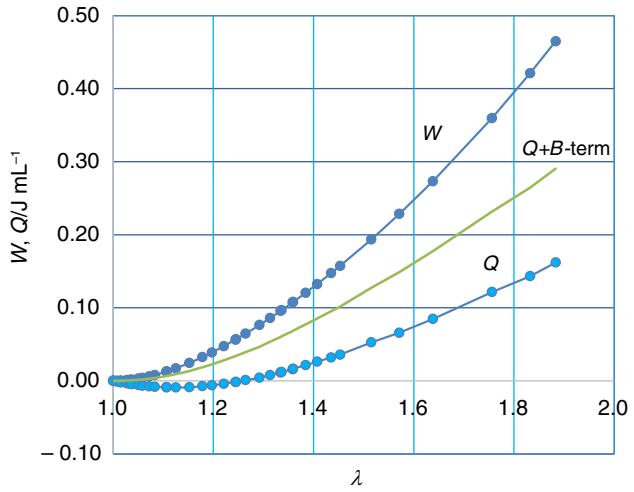

Fig. 14 Comparison of the work W and heat Q involved in extension of Silicone Rubber 1. W: work done on the rubber, Q: reversible heat generated during adiabatic extension. The difference W-Q is equal to the increase in the internal energy. The curve $Q+B$-term shows Q to which the heat calculated from the endothermal B-term of the entropy has been added. Data: PDMSExthardAa01, 20220304

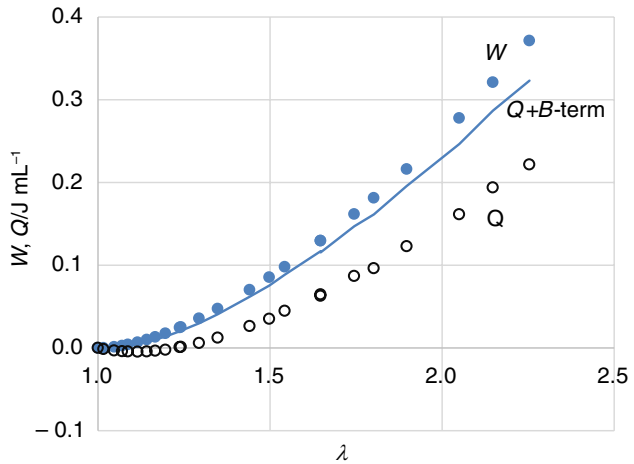

Fig. 15 Comparison of the work W and heat Q involved in extension of Silicone Rubber 2. W: work done on the rubber, Q: reversible heat given out during adiabatic extension. The difference W-Q is equal to the increase in the internal energy. The curve $Q+B$-term shows Q to which the heat calculated from the endothermal B-term of the entropy has been added. Data: pdmsBc07a sheet2, 20220411

The third curves in these figures, marked as $Q+B$-term, show an attempt to understand the large difference between the work W and the heat Q. These curves were calculated as follow. We have shown that the entropy of extension has two components, the endothermal and exothermal components corresponding to Eqs. 27 and 26, respectively. Actually measured temperature changes are resultant of these two. The exothermal effect is intrinsic to the rubber elasticity while the endothermal effect is a consequence of a more general property of condensed matter, related to thermal expansion and heat of compression. The basic idea is to calculate the amount of heat that we would observe if the endothermal effect were absent.

The heat associated with the endothermal effect was calculated by multiplying the B-term Eq. 27 by the temperature of the sample in the experiment. The heat thus calculated was added to the experimental value of the heat given by Eq. 31. The result would correspond to the intrinsic exothermal effect associated with the rubber elasticity. In this calculation, the B values from the fitting in the small λ region were used since they are more appropriate than those based on the larger λ regions for the present purpose of calculating the magnitude of the endothermal heat effect.

Figure 14 shows that about half of the W-Q difference of Silicone 1 is explained by the B-term. The B-term is more important in Silicone 2 as is shown in Fig. 15 where the heat corrected for the B-term (the curve marked as $Q+B$-term) lies close, though not exactly equal, to the experimental W curve.

A physical interpretation of this result would be that, if the heat absorption arising from the volume expansion that accompanies the mechanical elongation is corrected for, the rubber (Silicone 2) behaves like an ideal rubber. It should be noted that the heat absorption invoked here is a very general property of condensed matter. A substance with positive thermal expansivity absorbs heat when stretched. It is the reverse effect of the heating by compression.

The data shown in Fig. 14 and especially in Fig. 15 are reasonably well explained by the assumed mechanism. This may be used to determine the values of the expansion

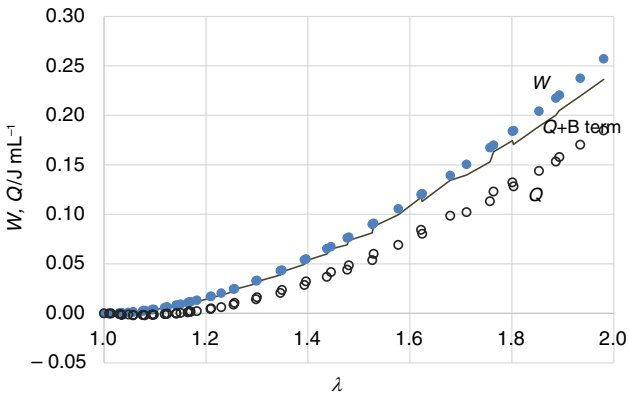

Fig. 16 Comparison of the work W and heat Q involved in the extension of natural rubber [22]. W: work done on the rubber, Q: reversible heat evolving during adiabatic extension. The difference W-Q is equal to the increase in the internal energy. The curve $Q+B$-term shows Q to which the heat calculated from the endothermal B term of the entropy has been added. Data: NRAjAkAmAnalysis, sheet2 20220106

coefficient, bulk modulus, and Poisson's ratio involved in the *B*-term in Eq. 27. Some of these are important in application and require a complicated experiment to determine.

The work *W* supplied to the natural rubber sample in its extension is also larger than the heat *Q* that evolves [22] just as we found in the present experiment with the silicone rubbers. The correction for the *B*-term, not considered in the paper [22], was applied to the published natural rubber data [22]. The corrected heat *Q* thus calculated is shown in Fig. 16 and is in nearly perfect agreement (~95%) with the mechanical work supplied. This agrees with the conclusion from previous works [8, 9] that the internal energy has only a minor role in the elasticity of natural rubber.

An interesting opposite case has been found in ethylene-propylene (EP) rubber in which more heat evolved than the mechanical work supplied [21]. This may be understood by assuming the extended state of ethylene-propylene rubber to be energetically more stable than in the normal state, a likely situation with these polymers whose melting temperatures (PE: 125 ℃, PP: 165 ℃) are considerably higher than the temperature at which the mechanocaloric experiment was performed. Thus the rubber at room temperature would retain a certain portion of the energy corresponding to the heat of melting. The structural randomness prohibits crystallization, but extension will introduce anisotropy in the local structure of the rubber that will facilitate mutual alignment of the polymer chains and lower the internal energy of the rubber. The interchain energy retained in the unstrained rubber will be released as the heat in the mechanocaloric experiment. This may explain the heat that exceeds the mechanical work supplied to the sample in the mechanocaloric measurement on EP rubber.

If the interchain attraction is strong enough, the tension may induce the EP rubber to crystallize in spite of the structural disorder. If this occurs, the heat that evolves during extension may be described as the heat of crystallization. Crystallization has actually been reported to take place by DSC, stress–strain relations, thermoelasticity, X-ray diffraction and other methods [26]. But the results are complicated with different samples behaving differently depending in particular on the cross-linking agent employed in the sample preparation. Crystallization is observed at higher extensions of $\lambda = 7.50$ [27]. For natural rubber, the measurement of the mechanocaloric response allowed to conclude that it crystallizes at extension $\lambda = 4.37$ at 30.0 ℃ [28]

The temperature of melting of silicone rubber is 235 K, much below the temperature at which we performed the experiment. There will thus be no possibility for the heat of melting to contribute to the heat of extension of silicone rubber.

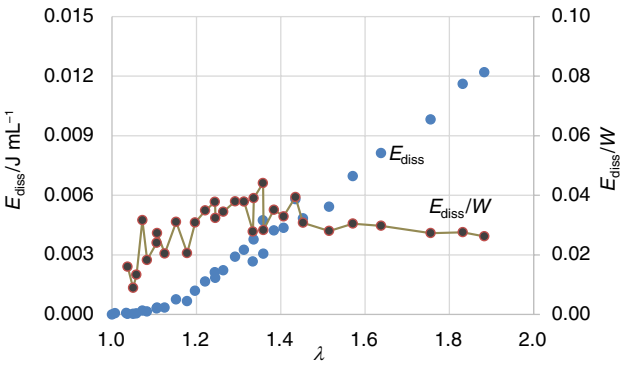

Fig. 17 The energy per unit volume dissipated in the extension of Silicone Rubber 1 to λ at 294 K (blue circles, left scale) and its ratio to the mechanical work expended for the extension (black circles, right scale). Data: PDMSExthardAa01a, 20220304

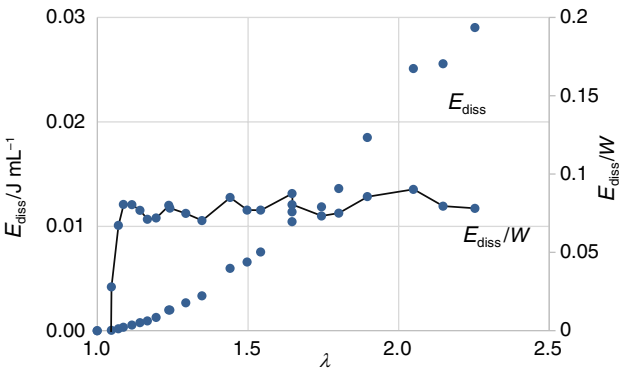

Fig. 18 The energy per unit volume dissipated in the extension of Silicone Rubber 2 to λ at 294 K (blue circles, left scale) and its ratio to the mechanical work expended for the extension (black circles, right scale). Data: pdmsBc07a, sheet2, 20220411

Irreversibilities in extension/contraction

We have pointed out in relation to Fig. 6 that the increment of the temperature $\Delta_1 T$ accompanying the extension of the rubber is larger than the decrement $\Delta_2 T$ accompanying its contraction (Figs. 7 and 9). The difference has been attributed to dissipation of the mechanical energy into heat. The dissipated energy $E_{\mathrm{diss}}(\lambda)$ can be calculated for a unit volume of the rubber by multiplication by the heat capacity density $c_{\lambda,\mathrm{V}}$.

$$E_{\mathrm{diss}}(\lambda) = c_{\lambda,\mathrm{V}}(\Delta_1 T(\lambda) - \Delta_2 T(\lambda))/2 \tag{32}$$

The factor 1/2 is inserted here to make the definition appropriate to the one-way deformation (extension or contraction).

Figure 17 and Fig. 18 show $E_{\rm diss}(\lambda)$ for Silicone 1 and Silicone 2, respectively. The ratios $E_{\rm diss}(\lambda)/W(\lambda)$ are also shown. The dissipation $E_{\rm diss}(\lambda)$ increases steadily as λ increases for both Silicone 1 and Silicone 2. But interestingly the ratio $E_{\rm diss}(\lambda)/W(\lambda)$ remains approximately constant for both of the samples. The ratio is about 0.03 for Silicone 1 and 0.08 for Silicone 2. As energy dissipation is a property that depends on various rate processes in rubber, it should be pointed out that the results in Figs. 17 and 18 were obtained with the rate of extension $\mathrm{d}\lambda/\mathrm{d}t = 0.04/\mathrm{s}$ typically. We do not understand at present the physical origin of the energy dissipation. We do not understand why the softer sample Silicone 2 is more dissipative than the hard Silicone 1 in the absolute value $E_{\rm diss}(\lambda)$ as well as in the ratio $E_{\rm diss}(\lambda)/W(\lambda)$. The present apparatus may be used to measure the dissipated energy quantitatively for different λ and $\frac{\mathrm{d}\lambda}{\mathrm{d}t}$ as well as for different pre-conditioning of the sample.

Conclusions

Sensitive and stable DC amplifiers that have become available recently at a relatively low cost, combined with computer-controlled digital instruments, have made a thermocouple an ideal thermometer for investigation of mechanocaloric properties of rubbers in which the time-varying temperature of the sample is measured while the sample undergoes extension and contraction by an external force. We have utilized this and made an easy-to-use apparatus for this type of experiment. A unique feature of the experiment is that the mechanical work done on the sample and the heat generated while the work is done are measured simultaneously. For two types of silicone rubbers of different hardness we examined, the engineering stress and entropy of extension gave mutually consistent number densities of the partial chains forming the elastomers. As to the comparison of the work done in extension and the heat that evolved, the work considerably exceeded the heat generated. A large part of the difference between the two energy components is explained by the endothermal term derived from the analysis of the entropy of extension. A tentative conclusion from the experiment is that real rubbers may be more close to ideality than the large difference between the work and heat suggests. We should probably examine the concept of the non-ideality of rubber more in detail at the thermodynamic and statistical mechanical levels than we do at present. We have shown that energy dissipation taking place in rubber while it is deformed can be quantified by our method of investigation. There would be a large number of experimental conditions which can be varied in the measurement of dissipative properties, but we did not consider them in this paper. They are, e.g., the time rate of deformation and the prehistory of the sample, in addition to the magnitude of the deformation. This need be done on a systematic planning of the experiment and will be a subject of a future study.

Acknowledgements We thank Professor emeritus A. Inaba, Graduate School of Science, Osaka University, for the heat capacity data of Silicone 2 and Professor Hal Suzuki, Department of Chemistry, Kindai University, for his kind help with the LabVIEW programming and for discussion of the experimental results. The authors are grateful to RCTES for supporting the present work.

Author contributions Takasuke Matsuo contributed to conceptualization and methodology, construction of the apparatus, execution of the experiment, analysis of the experimental data, interpretation of the results, writing the manuscript. Daisuke Takajo contributed to execution of the experiment, analysis of the experimental data, interpretation and discussion of the results, commenting on the manuscript.

Funding Open Access funding provided by Osaka University. This work is partially supported by RCTES Research and Education Funding.

References

1. Joule JP. On thermodynamic properties of solids. Phil Trans Roy Soc Lond. 1859;149:91–131.
2. Boone CE, Newman JR. Effect of heat generated during stressing upon the tensile properties of rubber. Ind Eng Chem. 1926;18:539–40.
3. Williams I. Transformation of energy by rubber. Ind Eng Chem. 1929;21:872–6.
4. Ornstein LS, Wouda J, Eymers JG. On the thermodynamics of caoutchouc. Proc Acad Sci Amst. 1930;33:273–9.
5. Dart SL, Anthony RL, Guth E. Rise of temperature on fast stretching of synthetics and natural rubber. Ind Eng Chem. 1942;34:1340–2.
6. Dart SL, Guth E. Rise of temperature on fast stretching of butyl rubber. J Chem Phys. 1942;13:28–36.
7. Peterson LE, Anthony RL, Guth E. Equation of state of some synthetic rubbers. Ind Eng Chem. 1942;34:1349–52.
8. Anthony RL, Caston RH, Guth E. Equation of state for natural and synthetic rubber-like materials.some synthetic rubbers. J Phys Chem. 1942;46:826–40.

9. James HM, Guth E. Theory of the elastic properties of rubber. J Chem Phys. 1943;11(455):481.
10. Shen MC, Mcquarrie DA, Jackson JL. Thermoelastic behavior of natural rubber. J Appl Phys. 1967;38:791–8.
11. Treloar RG. The Physics of Rubber Elasticity. 3rd ed. Oxford: Clarendon Press; 1975.
12. Doi M. Sofuto-mataa Butsurigaku Nyuumon (Introduction to Soft Matter Physics, in Japanese), Chapter 4, Iwanami, 2010, ISBN978–4–00–005616–8.
13. Doi M. Soft Matter Physics. USA: Oxford University Press; 2013.
14. Hanson DE. The distributions of chain lengths in a crosslinked polyisoprene network. J Chem Phys. 2011;134:064906–16.
15. Hanson DE, Barber JL, Subramanian G. The entropy of the rotational conformations of (poly)isoprene molecules and its relationship to rubber elasticity and temperature increase for moderate tensile or compressive strains. J Chem Phys. 2013;139:224906–16.
16. Hanson DE, Barber JL. A new paradigm for the molecular basis of rubber elasticity. Contemp Phys. 2015;56:319–37.
17. Koibuchi H, Bernard C, Chenal J-M, Diguet G, Srebald G, Cavaille J-Y, Takagi T, Chazeau L. Monte Carlo study of rubber elasticity on the basis of Finsler geometry modeling. Symmetry. 2019;11:1124–45.
18. Tomasz P, Kicior I. Pressure-freezing of dodecane: exploring the crystal structures, formation kinetics and phase diagrams for colossal barocaloric effects in n-alkanes. RSC Adv. 2023;13:33305–17.
19. Matsuo T, Inaba A, Yamamuro O, Hashimoto M, Sotani N. Rubber elasticity in the introductory thermodynamic course. J Therm Anal. 2003;69:1015–20.
20. Sakata A, Suzuki N, Higashiura Y, Matsuo T, Sato T. Measurement of the mechanocaloric effect in rubber. J Therm Anal Calorim. 2013;113:1555–63.
21. Matsuo T, Azuma N, Toriyama Y, Yoshioka T. Mechanocaloric properties of poly(dimethylsiloxane) and ethylene-propylene rubbers. J Therm Anal Calorim. 2016;123:1817–24.
22. Matsuo T, Suzuki H, Takajo D. High-resolution measurement of the mechanocaloric properties of natural rubber. Nihon Gomu Kyokaishi, 2022;95:212–218. (J. Soc. Rub. Sci. Tech. Jpn. 2022;95: 212–218. In Japanese).
23. Umeda M, Wakabayashi T, Kamiyama T, Suzuki H. Thermodynamic investigation on melting and recrystallization of poly (dimethylsiloxane) rubbers under strain. Polymers. 2022;254:125105.
24. Mott PH, Roland CM. Limits to Poisson's ratio in isotropic materials. Phys Rev B. 2009;80:132104–14.
25. Zemansky MW. Heat and Thermodynamics. McGraw-Hill: Inc; 1968. p. 306.
26. Scholtens BJR, Riande E, Mark JE. Crystallization in stretched and unstretched EPDM elastomers. J Polym Sci: Polym Phys Ed. 1984;22(1223):1238.
27. de Ballesteros OR, Auriemma F, Guerra G, Corradini P. Molecular organization in the Pseudo-hexagonal crystalline phase of ethylene propylene copolymers. Macromolecules. 1996;29:7141–8.
28. Matsuo T, Azuma N. Rubber elasticity in thermodynamics courses. Netsu Sokutei. 2016;43(W43E):1–10 ((**in English**)).